PERMAFROST AND PERIGLACIAL PROCESSES
Permafrost and Periglac. Process. **15**: 379–391 (2004)
Published online in Wiley InterScience (www.interscience.wiley.com). DOI: 10.1002/ppp.506

Development of Transverse Ridges on Rock Glaciers: Field Measurements and Laboratory Experiments

A. Kääb and M. Weber*

Department of Geography, University of Zurich, 8057 Zurich, Switzerland

ABSTRACT

Very high-resolution photogrammetric and geodetic measurements about the deformation of transverse ridges on Murtèl, Muragl and Suvretta rock glaciers in the Swiss Alps are discussed. The ridges are advected downstreams with a speed that equals the overall speed of the creeping permafrost within the significance level of the applied techniques. Any process of ridge formation is, thus, overlain on the mass creep. In fact, measurements yield local speed maxima on top of the ridges that can be explained by differential movement due to ridge growth through bulging under compressive flow. This hypothesis is consistent with results from laboratory experiments that were performed on a model ramp employing mixtures of Xanthan Gum, sand and gravel. Indications were also found that overthrusting is involved in the development of transverse ridges on rock glaciers. Copyright © 2004 John Wiley & Sons, Ltd.

KEY WORDS: rock glacier; creep; transverse ridges; folding; Swiss Alps

INTRODUCTION

The high thermal inertia of rock glaciers allows these frozen bodies to continuously deform and preserves their topography over centuries and millennia (Haeberli, 2000; Kääb *et al*., 2003). In addition, the content of solids and the ice-free, blocky active layer of rock glaciers contributes to the conservation of surface features even over periods of icemelt. The surface topography of rock glaciers cumulatively reflects the dynamic history and thus, in a complex way, their present and past internal conditions and environment. Transverse ridges and furrows represent the most prominent expression of rock glacier microtopography. Conclusions could be drawn about the dynamics of rock glaciers from interpreting their surface topography alone, once the processes that are involved in the evolution of such structures are understood. Furthermore, the decoding of the surface morphology contributes to the reconstruction of the dynamic and thermal history of rock glaciers (Frauenfelder and Kääb, 2000).

According to main hypotheses upon the transverse ridges and furrows on rock glaciers (cf. Whalley and Martin, 1992; Barsch, 1996), their formations might be attributed to:

— external factors, such as variations in debris input or climate conditions (cf. Olyphant, 1987; Barsch, 1996), or
— internal factors, such as the dynamic evolution of ridges under compression flow, or disturbance propagation from differential movement of discrete layers (e.g. Wahrhaftig and Cox, 1959; Potter, 1972; Haeberli, 1985; White, 1987; Loewenherz *et al*., 1989; Barsch, 1996; Kääb *et al*., 1998) (cf. also Fletscher, 1974; Fink, 1980).

* Correspondence to: Andreas Kääb, Department of Geography, University of Zurich-Irchel, Winterthurerstrasse 190, CH-8057 Zurich, Switzerland. E-mail: kaeaeb@geo.unizh.ch

Received 4 March 2004
Revised 16 August 2004
Accepted 23 August 2004

In addition, it is as yet unknown whether transverse ridges and furrows represent:

— dynamic structures, e.g. forming from emergence under compression flow regime (i.e. active formation), or if these forms are
— thermally shaped due to, for instance, differential melt (thermokarst) or frost heave processes (i.e. passive formation).

It is important to note that these four elements of hypotheses do not necessarily contradict each other. One possible process might enhance the other, or a combination might be necessary for the formation of micro-topographic structures.

In this contribution, the dynamics of transverse ridges on three rock glaciers in the Swiss Alps are examined using photogrammetry and terrestrial surveying. The focus of the investigations is on the development of individual ridges rather than on the general distribution of ridge zones and their spatio-temporal context within the rock glacier evolution (for investigations of the latter kind see Weber, 2003.) In addition, qualitative laboratory experiments are applied in order to evaluate the potential of such tests for detecting and understanding possible mechanisms of transverse ridge formation, and in order to initially inter-compare the findings from field work and remote sensing to laboratory tests.

Rock glaciers and their surface features develop very slowly. Very-high-precision methods are, thus, necessary to monitor related processes. A further aim of this study is, therefore, the evaluation of a set of measurement and analysis methods for the detailed examination of ridge formation on individual rock glaciers.

After description of the methods used, the results of the field measurements at Murtèl, Muragl and Suvretta rock glaciers in the Upper Engadine, Swiss Alps, and the results of the laboratory experiments are discussed. The contribution terminates with the presentation of two hypotheses about transverse ridge development on rock glaciers.

METHODS

Photogrammetry

High-precision surface kinematics of all three rock glaciers investigated here were measured on the basis of aerial photography of approximately 1:6000 to 1:8000 scale. The data were either obtained as complete area-wide three-dimensional surface velocity fields or in the form of longitudinal profiles. For this purpose, changes in permafrost thickness were computed from multi-temporal, i.e. repeated digital terrain models using standard procedures of analytical photogrammetry (Kääb *et al*., 1997) and digital photogrammetry (Kääb and Vollmer, 2000). Horizontal displacements were measured employing special techniques of analytical and digital photogrammetry (simultaneous monoplotting using multi-temporal stereo models, Kääb *et al*., 1997; digital image matching, Kääb and Vollmer, 2000). The accuracy of individual measurements of both changes in thickness and horizontal displacements is in the order of ± 2 cm a^{-1} root mean square, depending on the image scale and the period between the photo acquisitions.

Terrestrial Surveying

At Muragl and Suvretta rock glaciers, the deformation of individual ridges was observed along longitudinal profiles that consist of a number of small measurement marks placed on top of prominent blocks. The three-dimensional positions of these marks were surveyed in summer 2001 and summer 2002 through polar survey (combined triangulation and laser ranging) using an electronic, automatic total station (theodolite with included laser ranger, servo motors and automatic target recognition; TCA 1102 by Leica Geosystems). For each year and profile, the measurements were conducted, for the most part, twice from different instrument locations. The resulting redundant measurements led to an improved position error for individual marks in the order of ± 5 mm.

In addition to the three-dimensional positions from polar survey, the elevation of the measurement marks was also determined by optical levelling. From the known precision of the method and redundant measurements for the rock glaciers investigated here, an accuracy of $\pm$ 1–2 mm is estimated for an individual mark elevation. In the further analysis, the elevation obtained from polar survey was replaced by the (more accurate) elevation from optical levelling in order to combine the two measurement results (details on the measurement and transformation of results can also be found in Weber, 2003).

Kinematic Boundary Condition at the Surface

The photogrammetric and geodetic measurements of this study were quantitatively analysed on the basis of mass conservation, which can be expressed by the kinematic boundary condition at the surface (Hutter,

1983; Paterson, 1994; Kääb and Funk, 1999; Kääb, 2004). For a longitudinal profile, the relation is

$$\frac{\partial z^s}{\partial t} + v_x^s \frac{\partial z^s}{\partial x} - v_z^s - b = 0 \quad (1)$$

where b is mass balance at the surface, z^s is surface elevation, $\partial z^s/\partial t$ is change in surface elevation with time, $v_x{}^s$ is the longitudinal horizontal surface velocity component of a three-dimensional velocity vector $\boldsymbol{v} = (v_x, v_y, v_z)^T$, $\partial z^s/\partial x$ is the surface slope component in flow direction, and v_z^s denotes vertical velocity at the surface. The latter is

$$v_z^s = v_x^b \frac{\partial z^b}{\partial x} - \int_{z^b}^{z^s} \dot{\varepsilon}_{zz}\, \mathrm{d}z \quad (2)$$

where v_x^b denotes the horizontal velocity at a basal layer with elevation z^b, and $\dot{\varepsilon}_{zz} = \partial v_z/\partial z$. In the kinematic boundary condition at the surface equations (1) and (2) change in elevation. Surface slope, and horizontal and vertical velocity, can be measured on the basis of photogrammetric and geodetic techniques.

Laboratory Experiments

In order to evaluate the potential contribution of laboratory experiments to the understanding of transverse ridge formation on rock glaciers, a corresponding qualitative test series was conducted. It should be stressed in advance that these investigations did neither apply any scaling laws for physical modelling nor consider any rheological parameters. The aim of the experiment was rather to initially and qualitatively test potential experimental settings and test fluids.

As a model device, a ramp of two components was constructed: a tilted part of variable slope (mostly around 30°) and an horizontal ramp foot. On top of the slope a storage system was attached which allowed a defined release of the model mass.

The food additive Xanthan Gum (E415) was used as basic material of the model mass. Xanthan Gum is a microbial polymer produced in a pure culture fermentation of the bacterium Xanthomonas Campestris. The molecular structure of Xanthan Gum results in pseudo-plastic flow behaviour. For the actual model mass, mixtures of Xanthan Gum powder, water, sand and gravel were prepared. Density and viscosity were systematically varied from model run to model run, but also within an individual model mass mixture. By this procedure, the influence on ridge formation from (1) overall mass density and viscosity, and (2) density and viscosity gradients within the mass were explored (Weber, 2003; Weber and Kääb, 2003).

The model results were documented by repeated images using a fixed digital camera with vertical optical axis, i.e. providing nadir imagery. For selected model runs, surface displacements were measured by image matching techniques as described above (see section on photogrammetry) (Kääb and Vollmer, 2000). As yet, only one camera was employed. Therefore it was not possible to derive elevation models in addition to the displacements. For the same reason, the obtained displacements are not strictly horizontal but rather perpendicular to the individual camera projection vectors. In addition to the vertical imagery from a fixed camera position, various oblique images were taken for documentation using a second, handheld, digital camera.

RESULTS FOR MURTÈL ROCK GLACIER

Photogrammetric Profile

The evolution of micro-topography on Murtèl rock glacier is described in Kääb *et al.* (1998). A summary and some new aspects relevant here are given in the following for the sake of completeness and comparison. The results were obtained from a photogrammetric longitudinal profile (Figure 1) of surface geometry and velocity with 1 m horizontal spacing, and depicted in Figure 2. Also displayed are terms of the kinematic boundary condition at the surface equations (1) and (2): horizontal velocity, change in elevation and the product of surface slope times speed $(v_x^s \cdot \partial z^s/\partial x)$.

Over the investigated period 1986–1997, the horizontal creep rates at the surface amount to $0.16\,\mathrm{m\,a^{-1}}$ in the steep upper part and decrease to about $0.05\,\mathrm{m\,a^{-1}}$ in the flat lower part. The observed velocity increase at the rock glacier front may be related to the increase in slope. However, the measurements might also be affected to some extent by debris sliding along the surface down the front (cf. Koning and Smith, 1999; Kääb and Reichmuth, 2005, in press). The elevation changes reveal for the most part a constant term of about $-0.03\,\mathrm{m\,a^{-1}}$ in decrease of permafrost thickness, overlain by high-frequency variations. These variations clearly coincide with the product of surface slope and horizontal speed, which describes the effect of topography advection equation (1). The transverse buckling becomes first visible in the profile at approximately point $x = 150$ m. However, the point of first appearance of the structures needs not necessarily be the zone of their origin.

Geophysical soundings and drillings on Murtèl rock glacier (e.g. Haeberli *et al.*, 1998; Kääb *et al.*,

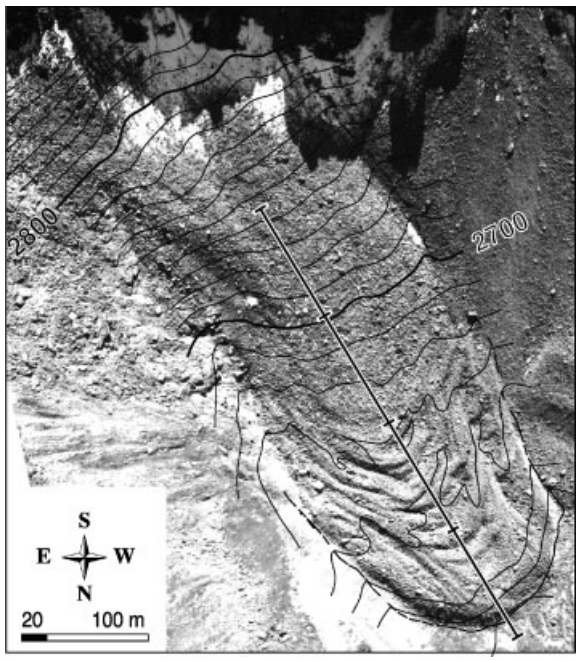

Figure 1 Ortho-image of Murtèl rock glacier in the Upper Engadine, Swiss Alps, from 11 September 1996. The straight line indicates the position of the profile shown in Figure 2. Aerial photograph taken by the Swisstopo flight service.

1998; Arenson *et al*., 2002; Vonder Mühll *et al*., 2003) revealed an active layer consisting of coarse blocks up to several metres in diameter. The thickness of the active layer ranges from 5 m within the ridges down to about 0.5 m in the furrows. The undulations are for the most part limited to the active layer, although the underlying massive ice layer is also affected to some extent. This ice layer, of over 90% ice content by volume, reaches down to a depth of about 28 m. Two thirds of the horizontal deformation of the permafrost column is concentrated within a layer of sandy ice reaching from about 28–30 m depth. Below this point, a non-deforming mixture of ice and coarse blocks can be found down to the permafrost base at around 55–60 m. Permafrost temperature is down to nearly −3°C.

The Murtèl measurements discussed here show that:

— The longitudinal horizontal surface velocities vary over the ridges in a way that maximum speeds are found on top of the ridges and minimum speeds in the furrows. The variations in speed thus clearly reflect the ridge and furrow topography.
— Regarding their average speed the distinct ridges that are up to 7 m high are advected downstream with a speed that approximates the overall speed of the entire permafrost body.
— Their formation zone seems to correlate with a distinct decrease in slope, but is also situated in a zone of compressive flow.
— The ridges continuously grow under a compressive flow regime.
— They seem to decay again towards the front where a short zone of longitudinal extension can be found.

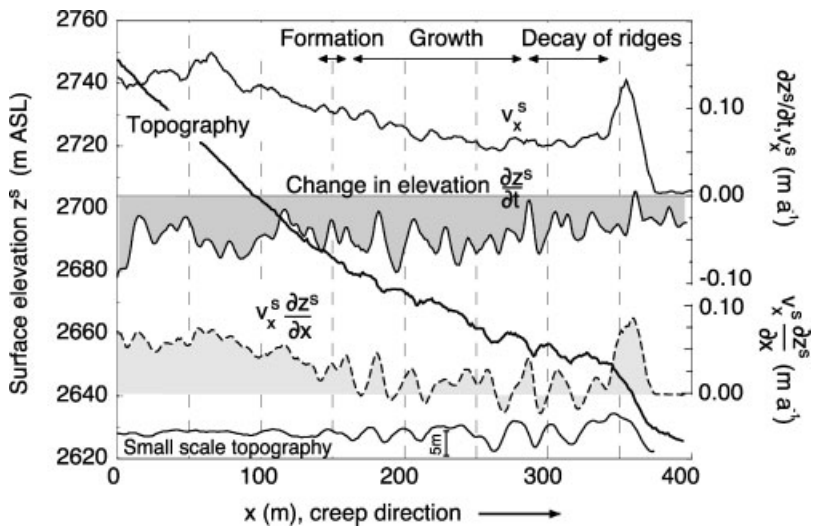

Figure 2 Longitudinal profile of rock glacier surface, surface velocities and derived kinematic quantities, 1987–1996, on Murtèl rock glacier. The photogrammetric profile measurements have a spatial resolution of 1 m. Surface topography is depicted with two times exaggeration. Small-scale topography is defined as the difference between surface topography at each point and a running average over 200 m (four times exaggeration). For profile location see Figure 1. (After Kääb *et al*., 1998.)

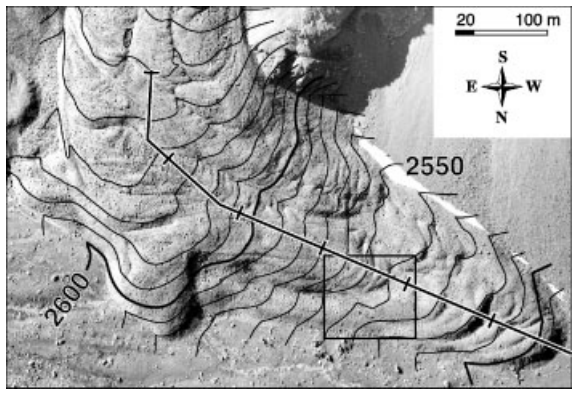

Figure 3 Ortho-image of Muragl rock glacier in the Upper Engadine, Swiss Alps, from 23 August, 1994. The rectangle to the lower right marks the section depicted in Figure 5. For the longitudinal profile see Figure 4. Aerial photograph taken by the Swisstopo flight service.

— The age difference between individual ridges is in the order of 300–400 a, as calculated from streamlines (Kääb *et al*., 1998; Haeberli *et al*., 1999).
— The horizontal compression in the order of $0.001\,a^{-1}$ found at the zone of ridge growth could theoretically be responsible for a surface uplift over time in the order of the observed ridge heights (vertical extension of $0.001\,a^{-1}$ over a 30 m thick (Arenson *et al*., 2002) incompressible ice slab results in about $+0.03\,m\,a^{-1}$ thickness increase.)

RESULTS FOR MURAGL ROCK GLACIER

Photogrammetric profile

A profile similar to that for Murtèl rock glacier was also measured for Muragl rock glacier for the period 1981–1994 (Figures 3 and 4). Because Muragl rock glacier is dynamically much more complex than Murtèl rock glacier, the profile includes several individual flow lobes (cf. Frauenfelder and Kääb, 2000). Accordingly, the horizontal velocities reflect rock glacier parts of different activity with maximum average speeds of $0.45\,m\,a^{-1}$. The small-scale topography includes typical transverse ridges and furrows (e.g. at around $x = 350$ m) as well as significantly larger fronts of individual flow lobes or rock glacier generations (e.g. from $x = 400$ m to $x = 550$ m). No overall trend of thickness change can be observed. The high-frequency changes of permafrost thickness correspond well with the calculated topography advection $(v_x^s \cdot \partial z^s/\partial x)$.

Geophysical soundings and drillings (e.g. Vonder Mühll, 1993; Arenson *et al*., 2002; Vonder Mühll *et al*., 2003) gave an active-layer thickness of about 2–7 m, and up to 20 m behind the front. The typical diameter of the surface debris is 0.5–1.5 m. At the drill sites (Figure 5), the active layer is underlain by about 15 m of blocks, gravel and sand with ice. The most part of horizontal deformation is concentrated at the bottom of this layer, which overlays the permafrost base. The permafrost temperature is close to 0°C, the ice content around 40–90% by volume.

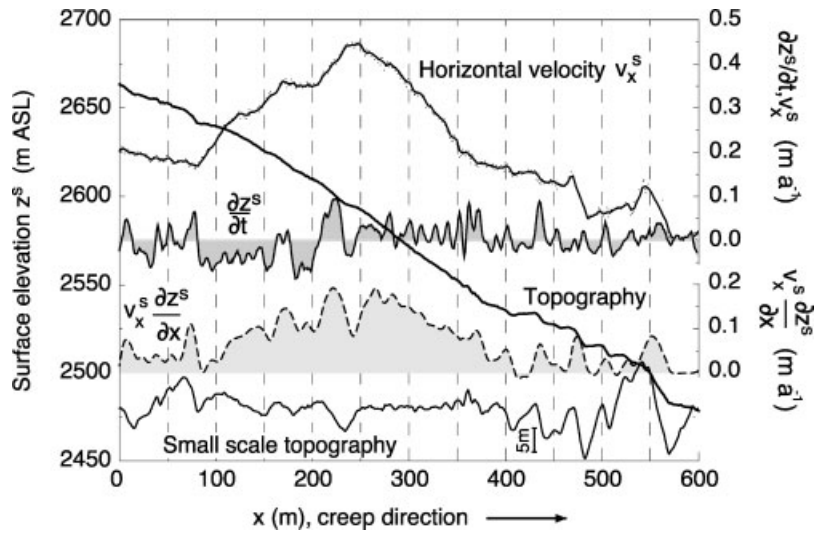

Figure 4 Muragl rock glacier: longitudinal profile of rock glacier surface, surface velocities and derived kinematic quantities, 1981–1994. For description, see the caption of Figure 2. For profile location, see Figure 3.

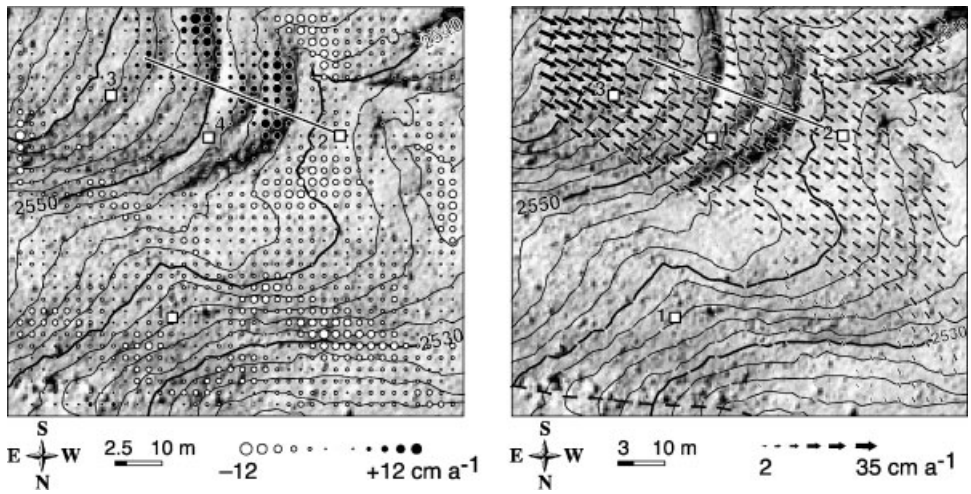

Figure 5 Permafrost thickness changes with 2.5 m (left) and 3 m (right) spaced horizontal displacements measured for a section of Muragl rock glacier between 1981 and 1994 (for location see Figure 3). The small rectangles indicate the location of boreholes no. 1–4 (cf. Arenson *et al*., 2002). The straight line marks the position of the profile shown in Figure 6. Ortho-image based on photography taken by Swisstopo flight service. (From Kääb and Vollmer, 2000.)

The Muragl photogrammetric measurements show:

— As for Murtèl rock glacier, the ridges that are up to 2 m high are advected downwards with a speed similar to the overall speed of the permafrost body.
— Their formation and growth take place in zones of strong longitudinal compression in the order of $-0.003\,\mathrm{a}^{-1}$, and well above a zone of slope decrease. The ridges show a continuous increase in size over a compression zone.
— As for Murtèl rock glacier, local speed maxima are found on top of the ridges, speed minima at furrows.
— The age difference between individual ridges is in the order of 50–70 a, as calculated from streamlines (Frauenfelder and Kääb, 2000).
— As for Murtèl rock glacier, the order of horizontal compression of roughly $-0.003\,\mathrm{a}^{-1}$ found in the zone of ridge growth could theoretically be responsible for a surface uplift in the order of the observed ridge heights (vertical extension of $0.003\,\mathrm{a}^{-1}$ over a 15 m thick (Arenson *et al*., 2002) incompressible ice slab results in $+0.04\,\mathrm{m\,a}^{-1}$ thickness increase).

Figure 5 depicts high-resolution measurements of horizontal surface velocities and thickness changes during 1981–1994 for the ridge-and-furrow zone around $x = 350$ m. South of boreholes 3–4–2, the results illustrate small-scale variations of thickness change from mass advection and an overall thickness increase of roughly $+0.02\,\mathrm{m\,a}^{-1}$ overlying each other (perhaps from compression or overthrusting?) (Kääb and Vollmer, 2000).

Geodetic Profile

From summer 2001 to summer 2002 high-precision terrestrial measurements of three-dimensional surface velocities were performed for a longitudinal profile south of boreholes 3–4–2 (Figure 5) (Weber, 2003). The repeated position of marks on boulders was determined by two-way close-range polar survey and optical levelling (see above section on methods). Figure 6 shows the topography, the horizontal and vertical velocity components obtained, and terms of the kinematic boundary condition equation (1). Note that the vertical velocity component is not equivalent to the horizontally fixed thickness change as obtained from photogrammetry $(\partial z^s/\partial t)$, but rather linked to the three-dimensional travel of an individual surface particle (v_z^s; cf. equation 2). The measurements and calculations reveal among other findings:

— Horizontal speeds (v_x^s) stay constant or even increase slightly on top of transverse ridges (cf. Figures 2 and 4). At the front of the ridges, speed partially decreases more strongly than the overall horizontal speed decrease observed for the profile. In sum, local speed maxima are found on the ridges.
— The vertical velocities (v_z^s) show no distinct small-scale variations. They increase longitudinally in

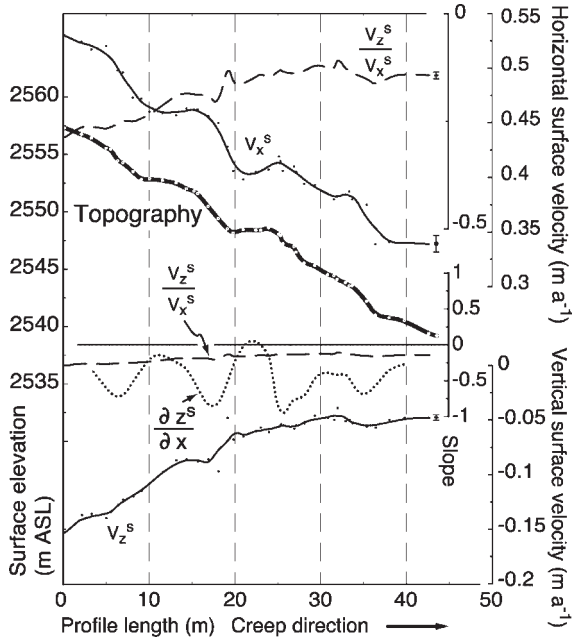

Figure 6 Muragl rock glacier: longitudinal high-precision profile of rock glacier surface, horizontal and vertical velocities, and derived kinematic quantities for 2001–2002. The data are obtained from polar survey and optical levelling. v_x^s: horizontal velocity at surface; v_z^s: vertical velocity at surface; $\partial z^s/\partial x$: surface slope. The slope of surface particle movement v_z^s/v_x^s is depicted twice with different vertical scales. Small dots indicate the raw measurements. Solid lines are interpolated by a running mean. Error bars to the right indicate the measurement accuracy. For profile location see Figure 5.

the upper part of the profile but stay nearly constant in the lower part.

— The surface slope $(\partial z^s/\partial x)$ is clearly different from the slope of the particle displacement (v_z^s/v_x^s). This fact shows that the surface velocity is not parallel to the surface but rather to a smooth layer at depth. This finding coincides perfectly with observations from borehole inclinometry in the area. Arenson *et al*. (2002) found a shear horizon in about 15 m depth.

— The slope of particle displacement is, furthermore, not constant but decreasing from −0.28 (−16°) to about −0.12 (−7°), while the overall surface slope is basically constant at −0.5 (−25°) (slope is calculated in creep direction, i.e. negative for longitudinally decreasing elevation). Thus, the shear horizon seems to emerge significantly towards the surface along the profile. The deformation measurements in boreholes 3 and 4, which are situated near the upper half of the surface profile (cf. Figure 5), did indeed yield downslope of approximately −0.31 (−18°) for the 2 m thick shear horizon at ca. 15 m depth (Arenson *et al*., 2002). The displacement slope for surface particles in the same zone calculated from the profile averages about −0.22 (−13°), i.e. approximately 5° less steep than the slope of the actual shear horizon.

— The overall increase in surface elevation $(\partial z^s/\partial t)$ observed from photogrammetry (Figure 5) appears, therefore, to be at least partially an effect of a mass-emergence component. The observed three-dimensional particle displacement is the resultant of (1) basal slope and speed, (2) mass balance, and (3) straining equations (1 and 2). All three processes could affect the calculated emergence velocity of about 0.13 m a^{-1}. From the above-mentioned borehole measurements, the emergence-velocity component due to basal sliding alone can be expected to be in the order of 0.09 m a^{-1}. The remaining difference compared to the measured emergence velocity could be the result of vertical extension or frost heave. The latter process is less likely for Muragl rock glacier, which is close to the melting point (cf. Arenson *et al*., 2002; Vonder Mühll *et al*., 2003).

— The shear horizon still exhibits significant small-scale topography; while its slope is roughly constant in the lower part of the profile, it decreases in the upper part. The shear horizon, therefore, seems to have a concave form.

RESULTS FOR SUVRETTA ROCK GLACIER

Geodetic Profile

Initial seismic and electric soundings available for Suvretta rock glacier (Vonder Mühll, 1993) reveal an active layer of 1–7 m thickness. Surface debris size varies from zones with coarse blocks of several metres in diameter to zones with fines and even humus with some vegetation. From the low elevation of the rock glacier permafrost temperature is believed to be warm.

A high-precision profile similar to that on Muragl rock glacier was measured on Suvretta rock glacier for 2001–2002 (Figures 7 and 8) (Weber, 2003):

— The investigated ridges lie in a zone of longitudinal compression in the order of 0.001–0.002 a^{-1}. Their age difference amounts to only about 20 years.

— Similar to Muragl and Murtèl rock glaciers, horizontal speed maxima are found on top or in the front slope of the individual ridges.

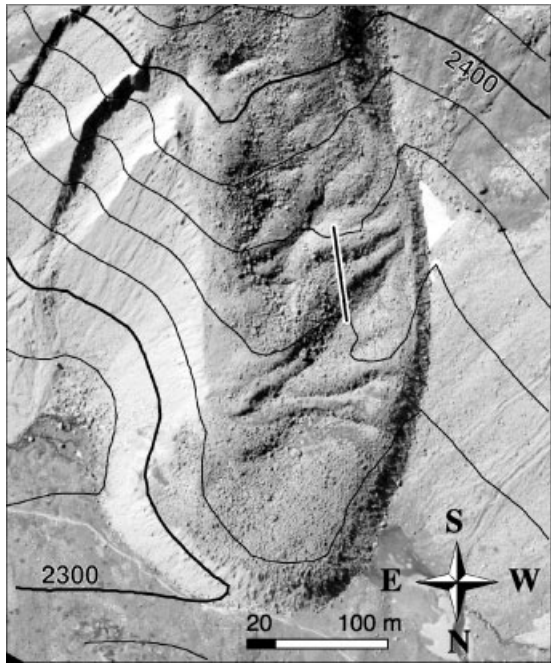

Figure 7 Ortho-image of Suvretta rock glacier in the Upper Engadine, Swiss Alps, from 16 September 1997. The straight line indicates the position of the profile shown in Figure 8. Aerial photograph taken by the Swisstopo flight service.

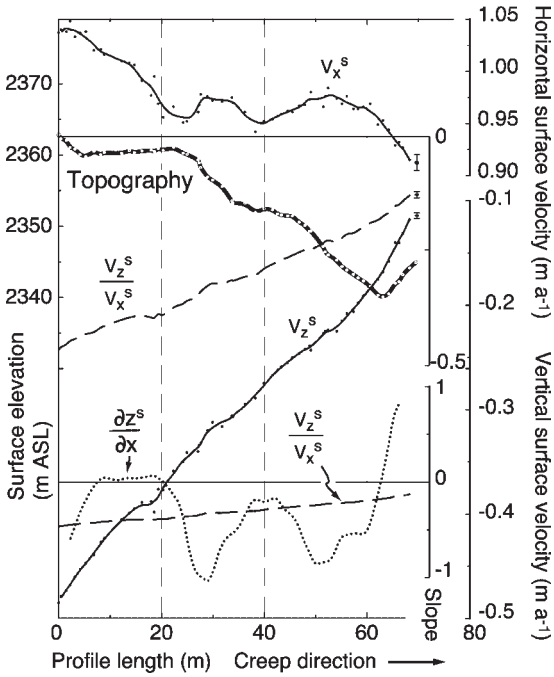

Figure 8 Suvretta rock glacier: longitudinal high-precision profile of rock glacier surface, horizontal and vertical velocities, and derived kinematic quantities 2001–2002. For description see the caption of Figure 6. For profile location see Figure 7.

— Both the vertical velocities and the particle displacement slope show no significant small-scale variations.
— Again, the three-dimensional particle displacement is not parallel to the surface. It is assumed, therefore, that a certain shear horizon exists within the observed section of Suvretta rock glacier.
— Such a potential shear horizon within Suvretta rock glacier shows no significant small-scale topography for the study site, as is to a certain extent apparent for Muragl rock glacier. The shear horizon does, however, also have a concave form with slopes of close to $-25°$ decreasing to about $-15°$.
— The slope of the shear horizon is not significantly different from the overall surface slope, which is very difficult to determine due to the coarse topography. Thus, it is not possible to detect an emerging or submerging flow component to a reliable degree.

LABORATORY EXPERIMENTS

For the physical experiments, Xanthan Gum (delivered as powder) was prepared with water until a suitable viscosity was obtained. For most model runs, sand and/or gravel were added, or different Xanthan/sand/gravel composites were mixed. In summary, the experiments showed the following qualitative trends (Figures 9–11):

— No, or only very minor, transverse ridges at or near the break of ramp slope were observed when the material was well mixed and 'homogeneous' (i.e. no solid content; pure Xanthan Gum fluid).
— If two Xanthan Gum fluids of different viscosity (i.e. different water content) but without solid content were only slightly mixed ('heterogeneous'), fine transverse ridges could develop near the break of slope. After sufficient material crept downwards and started to accumulate in the horizontal part of the ramp, ridges developed also above the break of slope.
— Ridges also developed when sand and/or gravel were added to a single-component mass.
— Distinct ridges appeared when two sand- and gravel-containing components with different viscosity were only slightly mixed or applied in two separate horizontal layers (Figure 9).
— In a final experiment series, a slightly mixed mass with sand and gravel ('heterogeneous') formed the bottom layer covered by a dry, brittle top layer of gravel (Figure 10). Distinct ridges developed for this model mass. Moreover, due to the

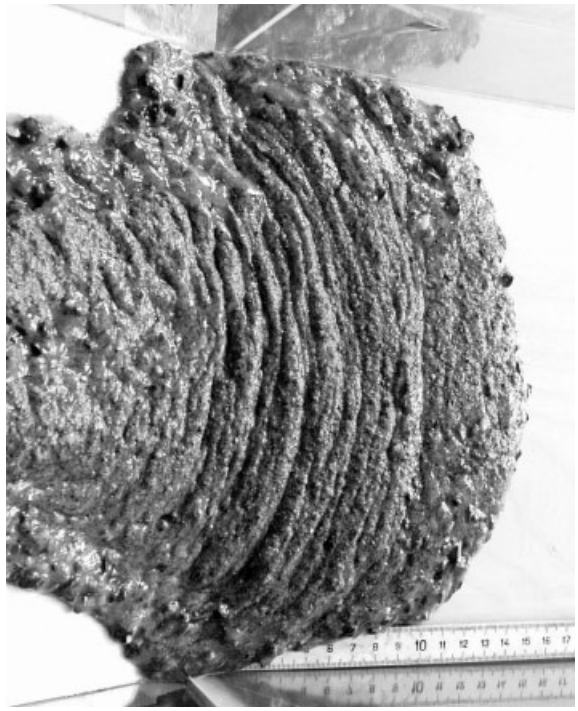

Figure 9 Oblique view of a part of the experimental ramp during a test for investigating the development of transverse ridges. In the model run shown, the model mass consists of a slightly mixed composite of sand- and gravel-containing Xanthan Gum fluids. The mass is flowing from left to right. The left third of the image depicts a part of the 30° ramp slope, the right two thirds the horizontal ramp foot. The corresponding break of slope is vertical in the image. Scale-bar sections to the lower right are in centimetres.

Figure 10 Oblique view of the horizontal ramp foot during an experiment using a slightly mixed mass comprising Xanthan, sand and gravel, covered by a brittle layer of dry gravel. The mass is flowing from the upper right to the lower left. Scale-bar sections to the lower left are in centimetres.

compression at the point of break in slope, viscous material was pushed from underneath towards, and through, the surface layer forming ridges of increasing amplitude. Gravel particles were dislocated and fell into the newly-formed furrows. A systematic sorting of the gravel particles was observed. In contrast to the above experiment series without dry top layer (Figure 9), this experiment yielded significantly larger wavelengths and amplitudes for the ridges (Figure 10).

In all experiments that showed surface folding, the ridges were largest around the break of slope and decayed again in flow direction (e.g. Figure 9). In the experimental setting used the authors consider the Xanthan/sand/gravel mixtures to reflect the entire deforming part of a rock glacier column. Only the final experimental series contained a brittle surface layer which was aimed to simulate the active layer.

From a sequence of vertical images of the final experiment with a dry top layer of gravel superimposed on the Xanthan/sand/gravel mixture (Figure 10) horizontal displacements were measured photogrammetrically (Figure 12). A distinct decrease in horizontal speed indicates strong compression. Local speed maxima can be found around the ridge tops.

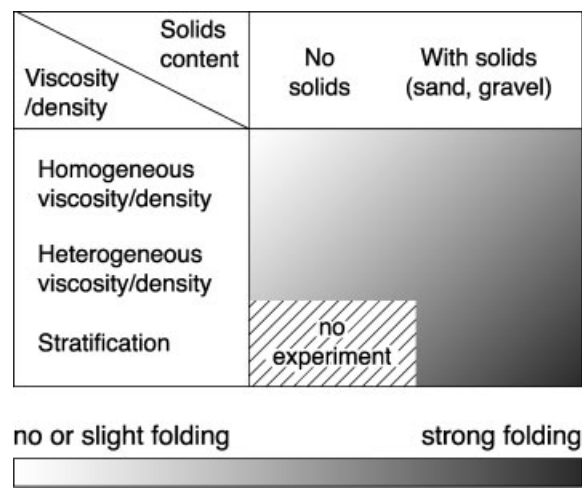

Figure 11 Qualitative scheme summarizing the influence of solid content and viscosity/density gradients within the model mass on the development of transverse ridges on the experimental ramp.

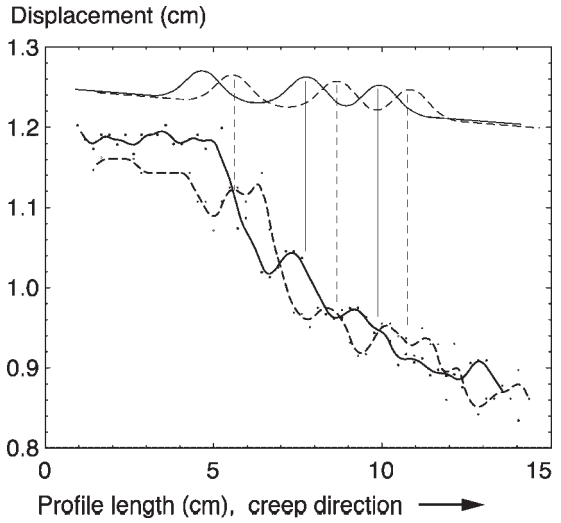

Figure 12 Longitudinal profile of approximately horizontal displacements on the surface of the model mass during the experiment (see Figure 10). Displacements have been measured only for the lower, horizontal part of the ramp. The solid line indicates the (interpolated) displacements between pictures i and i + 1, the dashed line between pictures i + 1 and i + 2. The small dots mark the original measurements. To the top of the figure, the average position of ridges between pictures i and i + 1 (solid) and pictures i + 1 and i + 2 (dashed) is schematically indicated. This topography is only qualitatively reconstructed from the vertical images, which also formed the basis for the displacement measurements.

DISCUSSION

The high-precision and high-resolution measurements for Murtèl, Muragl and Suvretta rock glaciers clearly indicate that the micro-topography on these rock glaciers is predominantly or even completely advected downstream, i.e. riding on the creeping bodies. Any process of ridge formation has to be superimposed on the overall permafrost creep. The photogrammetric and terrestrial measurements suggest that compressive flow does indeed play a role in the formation of transverse ridges (cf. Weber, 2003). The overall magnitude of permafrost creep and the degree of straining seem, furthermore, to affect the speed of ridge formation. Rock glacier dynamics and speed of ridge formation can be connected through rheological parameters.

The ridges observed for Murtèl, Muragl and Suvretta rock glaciers show considerable differences in wavelength and amplitude. Since it was out of the scope of this study, it becomes unclear whether these differences are due to different material properties or temporal scales involved.

For Murtèl, Muragl and Suvretta rock glaciers, horizontal speed shows local maxima on top of the ridges. Such variation in horizontal speed could theoretically reflect the flow of a mass over a basal bump or sticky spot (i.e. a geometric or friction obstacle, respectively) (Gudmundsson, 2003). However, in these cases the slope of particle displacement would have to reflect such passing over the obstacle. No significant variations in the slope of particle displacement along the profiles can be recognized in the presented terrestrial measurements. The possibility that the frozen mass overrides the ridges can thus be ruled out as far as the accuracy of the terrestrial measurements permits. Furthermore, the high redundancy of photogrammetric and geodetic measurement points allows us to exclude the possibility that the observed speed maxima are only due to unstable and individually displacing blocks. The photogrammetric measurements revealed a highly coherent surface flow field with no signs for shifting or rotating blocks. The scatter of the geodetic velocity measurements is within the level of measurement accuracy, i.e. no large individual movements of blocks could be found.

The laboratory experiments conducted in this study suggest that a heterogeneous variation of viscosity and/or density, including the content of solids, seems to favour or even to be a prerequisite for transverse folding. Such conditions are frequently found in rock glaciers, but not in debris-free glaciers which show no folding. A dry, brittle top layer, simulating the active layer in the laboratory experiments, seems to enhance transverse folding but is not a mandatory prerequisite for such a process. Quantitative conclusions about the influence of the thickness of such a dry top layer on the folding cannot be drawn from the tests. However, the laboratory experiments suggest that the degree of folding varies with mixture characteristics such as debris content and stratification, i.e. properties that influence the viscosity and/or density distribution within the deforming mass. Therefore, spatio-temporal variations in the rock glacier composition such as change in active layer thickness or change in ice content are likely to also affect transverse folding. Similarly, pre-existing layering, such as tilted layers found in several rock glaciers (e.g. Berthling *et al.*, 2000), is likely to influence transverse folding.

Local speed maxima on top of individual ridges were measured for the Xanthan Gum mass with a dry top layer of gravel as well as for the three rock glaciers investigated here. As for the rock glaciers investigated, the speed of ridge advection also approximates the overall surface speed for the physical models (Figure 12). This fact might point to similar ridge

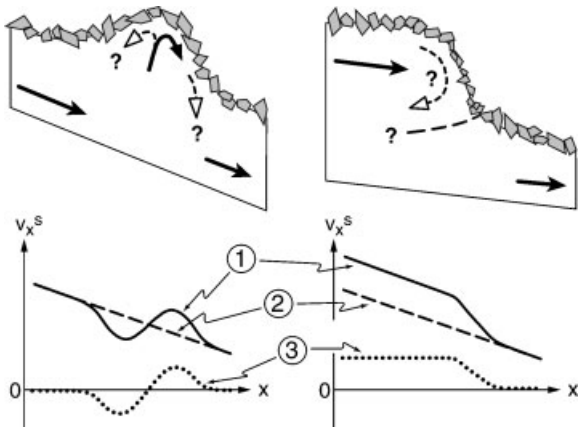

Figure 13 Two hypothetical processes for the formation of transverse ridges on rock glaciers. Left: bulging, right: overthrusting. The lower schemes show how the formation modes lead to different surface velocity profiles. (1) Actual surface velocities result from (2) the overall speed gradient (here: decrease) and (3) the relative speeds connected to ridge formation itself.

formation processes in the laboratory experiments and on rock glaciers.

From the measurements and the physical model presented here, two possible processes of ridge development can be deduced (Figure 13):

— Bulging: an active process of material uplift under a regime of compressive flow forms the ridges. This process leads to a relative negative speed-component (i.e. a speed-component in upstream direction) on the upstream part of the ridge, and to a relative positive speed-component for the downstream part. The resulting sum (1 in Figure 13) of two speed components, namely a general speed decrease (2 in Figure 13) and the ridge formation (3 in Figure 13), can then be observed at the surface as a local speed maximum on the ridges.
— Overthrusting: faster flow lobes override slower lobes from above. At individual ridges, or lobe fronts, processes similar to the ones taking place at the rock glacier front might occur ('conveyor belt' mechanism; Kääb and Reichmuth, 2005, in press).

The measurements and initial field interpretation show no clear indication for any of these hypotheses. For instance, no obvious changes in fines content were observed, potentially a sign for material uplift on the ridges. Moreover, both processes or parts of them seem to be in operation (cf. Wahrhaftig and Cox, 1959; White, 1987; Johnson, 1998). Overthrusting certainly plays a role for the large-magnitude surface undulations on Muragl (Figure 4) and Suvretta rock glaciers. On the other hand, the velocity profiles obtained for Murtèl (Figure 2) and Muragl (Figure 4) rock glaciers can hardly be explained by overthrusting alone. For the high-precision study site on Muragl rock glacier (Figures 5 and 6) some small-scale buckling seems to overlay a general overthrusting of the entire flow lobe onto a slower, less steep lower part of the rock glacier.

The measurements conducted within this study give no clear indication about the possible decay of transverse ridges by erosion or dispersion of the feature, or extensive flow regime. For the laboratory experiments dispersion of the ridges could be observed, in parts combined with erosion at the ridge flanks. Dispersion and/or flank erosion will act on the ridges in any case, possibly at time scales difficult to measure in nature. The degree of these processes is certainly increasing with the size and flank slope of the ridges. Under compressive flow above a certain rate, however, the ridge formation process is able to over-compensate these decay mechanisms. Extensive flow, on the other hand, seems to enhance the decay of the ridges. The maximum size of a ridge is believed to reflect the balance between ridge formation and decay processes. The intensity and temporal scale of both seem to vary for individual rock glaciers due to, for example, surface material, rheology and velocity.

The study presented here considered the formation of transverse ridges around a central flow line of a rock glacier. Towards the margins of a rock glacier transverse ridges are often deformed by the lateral speed decrease and may end up as nearly longitudinal ridges. The findings of this study are believed to apply in large parts also for lateral ridges of such kind because the largest compression at the lateral parts of a rock glacier is directed towards the margins, i.e. rotated in a similar way to the ridges.

CONCLUSIONS AND PERSPECTIVES

The photogrammetric and geodetic high-precision measurements of this study revealed clearly that transverse ridges and furrows on the rock glaciers investigated here are advected downstream with a velocity that equals the overall permafrost creep. Local speed maxima observed on top of individual ridges for all three rock glaciers are overlain onto the overall mass transport and are an indication of an active, dynamic ridge development. Saying that, the authors also favour rock glacier internal processes as main factors for the development of transverse ridges. Rock glacier external factors might nevertheless cause

disturbances such as viscosity and/or density contrasts, which then trigger these internal processes. That possibility, in particular, becomes evident if ridges develop from overthrusting which can, for instance, be the result of changes in speed and/or material supply.

Both the photogrammetric and geodetic measurements, and the laboratory experiments suggest that transverse ridges show a pattern of continuous growth downstream under compressive flow. That finding coincides well with previous suggestions by other authors (e.g. Wahrhaftig and Cox). A break in slope can be a reason for such compression but is not necessary *per se* for folding. Each individual ridge is subject to longitudinal compression with largest rates on the downslope part.

A thorough investigation of the two hypotheses presented above or the development of new ones will be possible from high-precision monitoring over longer time intervals than available here. The authors want to stress that the two processes of ridge formation discussed above are by no means exclusive or definite. Other processes might well be able to explain the observations. Further insights might be gained from comparing the ridge formation processes derived here with field surveys on variations in lichen cover or in grain size distribution and debris orientation.

The initial laboratory experiments conducted here turned out to be very promising. Although only meant to be qualitative, the tests showed clearly the influence of viscosity/density contrasts in the used mass on ridge development. Distinct variations in density and rheological properties within the mass favoured the formation of large ridges. As one of the most instructive observations, mass of a viscous bottom layer was pressed through a brittle, dry surface layer, actively forming transverse ridges at and below a sharp decrease in surface slope. The horizontal surface displacements obtained for that experiment are consistent with field observations.

The laboratory experiments suggest that spatio-temporal variations of rock glacier composition are likely to influence the formation of transverse ridges, and, in turn, that observed transverse folding can potentially be used to draw conclusions about the composition of rock glaciers.

The fact that the laboratory experiments presented here, and the terrestrial and remote sensing measurements for three rock glaciers with very different compositions and dynamics gave consistent results, suggest that the basic findings from this study might apply to other rock glaciers, or even form general characteristics of the development of transverse ridges on rock glaciers.

For the methodology, the results presented here show that high-precision and high-resolution measurements in combination with modelling work, e.g. based on the kinematic boundary condition at the surface, permit analysis of flow characteristics at depth, and assessment of the geometry of rock glacier shear horizons or other forms of bedding layers. Such an approach represents an efficient and simple complement to borehole experiments and geophysical soundings. A longitudinal profile or an entire field of three-dimensional high-precision surface displacements including both the rock glacier front and surface will make it possible to estimate the vertical velocity profile in the frontal part of the rock glacier (Kääb and Reichmuth, 2005, in press) and to follow, to a certain extent, the depth of a potential shear horizon or other deformation feature. Repeated digital photogrammetry of large-scale imagery or terrestrial laser scanning (Bauer *et al*., 2003) is, next to terrestrial surveying, also able to fulfil these requirements if surface particles are directly tracked in three dimensions.

ACKNOWLEDGEMENTS

Madlaina Perl, Edith Oosenbrug, Marcello Napoletano and Ivo Pfammatter supported the field measurements. Ivan Woodhatch helped to construct the experimental ramp. The company Stärkle & Nagler AG, Zollikon, Switzerland (Mr Strupler) provided the Xanthan Gum. We also want to thank the Swisstopo flight service for acquisition of the aerial photographs used in this study. Thanks are due to Wilfried Haeberli for his comments, and Susan Braun-Clarke for editing the English of an earlier version of the manuscript. The constructive and helpful reviews of two anonymous referees are gratefully acknowledged.

REFERENCES

Arenson L, Hoelzle M, Springman S. 2002. Borehole deformation measurements and internal structure of some rock glaciers in Switzerland. *Permafrost and Periglacial Processes* **13**(2): 117–135. DOI: 10.1002/ppp.414.

Barsch D. 1996. *Rock Glaciers. Indicators for the Present and Former Geoecology in High Mountain Environments*. Springer: Berlin.

Bauer A, Paar G, Kaufmann V. 2003. Terrestrial laser scanning for rock glacier monitoring. In *Proceedings, Eighth International Conference on Permafrost*, Zurich, Balkema, Lisse, 1, 55–60.

Berthling I, Etzelmüller B, Isaksen K, Sollid JL. 2000. Rock Glaciers on Prins Karls Forland. II: GPR

soundings and the development of internal structures. *Permafrost and Periglacial Processes* **11**: 357–369. DOI: 10.1002/ppp.366.

Fink J. 1980. Surface folding and viscosity of rhyolite flows. *Geology* **8**: 250–254.

Fletscher RC. 1974. Wavelength selection in the folding of a single layer with power-law rheology. *American Journal of Science* **274**: 1029–1043.

Frauenfelder R, Kääb A. 2000. Towards a palaeoclimatic model of rock glacier formation in the Swiss Alps. *Annals of Glaciology* **31**: 281–286.

Gudmundsson GH. 2003. Transmission of basal variability to a glacier surface. *Journal of Geophysical Research—Solid Earth* **108**(B5): art. no. 2253. DOI: 10.1029/2002JB002107.

Haeberli W. 1985. *Creep of mountain permafrost*. Mitteilungen der Versuchsanstalt für Wasserbau, Hydrologie und Glaziologie der ETH Zürich, 77. 142 pp.

Haeberli W. 2000. Modern research perspectives relating to permafrost creep and rock glaciers. *Permafrost and Periglacial Processes* **11**: 290–293. DOI: 10.1002/ppp.372.

Haeberli W, Hoelzle M, Kääb A, Keller F, Vonder Mühll D, Wagner S. 1998. Ten years after drilling through the permafrost of the active rock glacier Murtèl, Eastern Swiss Alps: answered questions and new perspectives. *Proceedings, 7th International Conference on Permafrost, Yellowknife*, Université Laval Press, Québec, Canada; 403–410.

Haeberli W, Kääb A, Wagner S, Geissler P, Haas JN, Glatzel-Mattheier H, Wagenbach D, Vonder Mühll D. 1999. Pollen analysis and 14C-age of moss remains recovered from a permafrost core of the active rock glacier Murtèl/Corvatsch (Swiss Alps): geomorphological and glaciological implications. *Journal of Glaciology* **45**(149): 1–8.

Hutter C. 1983. *Theoretical Glaciology; Material Science of Ice and the Mechanics of Glaciers and Ice Sheets*. D. Reidel Publishing; Terra Scientific Publishing Co, Dordrecht, Tokyo.

Johnson PG. 1998. Morphology and surface structures of Maxwell Creek rock glaciers, St. Elias Mountains, Yukon: rheological implications. *Permafrost and Periglacial Processes* **9**: 57–70. DOI: 10.1002/ppp.275.

Kääb A. 2004. *Mountain glaciers and permafrost creep. Research perspectives from earth observation technologies and geoinformatics*. Habilitation thesis. Department of Geography, University of Zurich.

Kääb A, Funk M. 1999. Modelling mass balance using photogrammetric and geophysical data. A pilot study at Gries glacier, Swiss Alps. *Journal of Glaciology* **45**(151): 575–583.

Kääb A, Reichmuth T. 2005. Advance mechanisms of rock glaciers. *Permafrost and Periglacial Processes*, in press.

Kääb A, Vollmer M. 2000. Surface geometry, thickness changes and flow fields on creeping mountain permafrost: automatic extraction by digital image analysis. *Permafrost and Periglacial Processes* **11**(4): 315–326. DOI:10.1002/ppp.365.

Kääb A, Haeberli W, Gudmundsson GH. 1997. Analysing the creep of mountain permafrost using high precision aerial photogrammetry: 25 years of monitoring Gruben rock glacier, Swiss Alps. *Permafrost and Periglacial Processes* **8**(4): 409–426.

Kääb A, Gudmundsson GH, Hoelzle M. 1998. Surface deformation of creeping mountain permafrost. Photogrammetric investigations on rock glacier Murtèl, Swiss Alps. *Proceedings, 7th International Permafrost Conference*, Yellowknife, Canada, Université Laval Press, Québec, Nordicana 57, 531–537.

Kääb A, Kaufmann V, Ladstädter R, Eiken T. 2003. Rock glacier dynamics: implications from high-resolution measurements of surface velocity fields. *Proceedings, Eighth International Conference on Permafrost*, Zurich, Balkema, Lisse, 1, 501–506.

Koning DM, Smith DJ. 1999. Movement of King's Throne rock glacier, Mount Rae area, Canadian Rocky Mountains. *Permafrost and Periglacial Processes* **10**(2): 151–162. DOI: 10.1002/ppp.312.

Loewenherz DS, Lawrence CJ, Weaver RL. 1989. On the development of transverse ridges on rock glaciers. *Journal of Glaciology* **35**(121): 383–391.

Olyphant GA. 1987. Rock glacier response to abrupt changes in talus production. In *Rock glaciers*, Giardino JR, Shroder JF, Vitek JD (eds). Allen & Unwin: Boston; 55–64.

Paterson WSB. 1994. *The Physics of Glaciers. Third edition*. Elsevier, Oxford, etc. 380 pp.

Potter N. 1972. Ice-cored rock glacier, Galena Creek, Northern Absaroka Mountains, Wyoming. *Geological Society of America Bulletin* **83**: 3025–3058.

Vonder Mühll D. 1993. *Geophysikalische Untersuchungen im Permafrost des Oberengadins*. PhD thesis, Versuchsanstalt für Wasserbau, Hydrologie und Glaziologie der ETH Zürich, ETH Zürich.

Vonder Mühll DS, Arenson LU, Springman SM. 2003. Temperature conditions in two Alpine rock glaciers. *Proceedings, Eighth International Conference on Permafrost*, Zurich, Balkema, Lisse; 2, 1195–1200.

Wahrhaftig C, Cox A. 1959. Rock glaciers in the Alaska Range. *Bulletin of the Geological Society of America* **70**: 383–436.

Weber M. 2003. *Oberflächenstrukturen auf Blockgletschern*. Diploma thesis, Department of Geography, University of Zurich.

Weber M, Kääb A. 2003. Laboratory experiments towards better understanding of surface buckling of rock glaciers. *Proceedings, Eighth International Permafrost Conference, Extended Abstracts*, Zurich, Balkeme, Lisse, 183–184.

Whalley WB, Martin HE. 1992. Rock glaciers. Part II: models and mechanisms. *Progress in Physical Geography* **16**(2): 127–186.

White SE. 1987. Differential movement across ridges on Arapaho rock glaciers, Colorado Front Range, US. In *Rock Glaciers*, Giardino JR, Shroder F, Vitek JD (eds). Allen & Unwin: London; 145–149.

